

Estimation Algorithm of Relative Position and Attitude during Proximity Rendezvous and Docking Using Multiple Ultra-Wide-Band Devices

By Mikihiro IKURA¹⁾

¹⁾ Department of Aeronautics and Astronautics, The University of Tokyo, Tokyo, Japan

This research proposes estimation algorithms of relative position and attitude during interplanetary proximity rendezvous and docking by using Ultra-Wide-Band (UWB) devices. The UWB device is a low-power and small communication device between several spacecraft, and it is suitable to mount micro spacecraft. It can be used for high precision ranging and high speed communication. In this paper, two estimation algorithms, which effectively use UWB's properties, are discussed. The first one estimates the relative position by using the ranging data of UWB devices and obtains the relative attitude information from the attitude sensors shared by the UWB communications. The second one assumes that the attitude sensor of the chaser cannot work, and the relative attitude is estimated by using the multiple ranging data of UWB devices. This research evaluates the observability and the estimation accuracy of the two proposed algorithms using a rendezvous simulator. This evaluation reveals the conditions of the relative position and attitude for the accurate and stable estimation. This paper will contribute to the maneuver planning of interplanetary proximity rendezvous and docking and will expand the capability of future deep space missions by micro spacecraft.

Key Words: Rendezvous and Docking, UWB device, Interplanetary Spacecraft, Kalman Filter

Nomenclature

L	:	position vector
q	:	quaternion
ω	:	angular velocity vector
F	:	force vector
T	:	torque vector
I	:	inertia tensor
M	:	mass of spacecraft
C	:	coordinate transformation matrix
U	:	position vector of UWB device

Subscripts

i	:	inertial frame
c	:	chaser
t	:	target
d	:	disturbance
m	:	input of control

1. Introduction

In recent years, technologies of micro spacecraft have been improved, and many earth orbiting satellites such as XI-IV, XI-V,¹⁾ and PRISM²⁾ were developed. Furthermore, the demonstration of PROCYON³⁾ certifies realization of deep space exploration by a single micro spacecraft, and many missions of interplanetary micro spacecraft are proposed. However, resources of the micro spacecraft such as propulsion and electric power are extremely limited, and future missions of a single micro spacecraft have some limitations.

A docking between large spacecraft which has a lot of resources, and micro spacecraft expands their mission capability more and more. For a demonstration of such docking system in deep space, medium spacecraft DESTINY+ are

proposed by JAXA. DESTINY+ mounts micro spacecraft PROCYON-mini⁴⁾ that is developed by the University of Tokyo. PROCYON-mini is taken to an asteroid by DESTINY+, separated to perform proximity flyby observation, and re-docked to DESTINY+ again to go to other asteroids. This rendezvous and docking system can realize a higher level mission in deep space by micro spacecraft.

PROCYON-mini uses UWB (Ultra-Wide-Band) devices for rendezvous sensors. The UWB device is a low power and small communication system and is able to be high-accuracy ranging and high-speed communication simultaneously. The UWB device is suitable for rendezvous sensor of micro spacecraft because of their limitation of resources.

One of the goals of this research is to propose estimation algorithms of relative position and attitude during proximity rendezvous and docking by using multiple UWB devices in order to realize DESTINY+ and PROCYON-mini project.

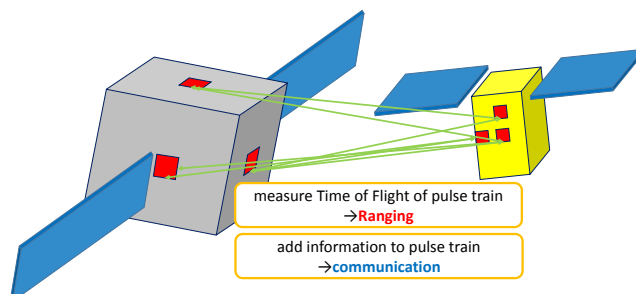


Fig. 1. Overview of rendezvous and docking with UWB devices

2. Ultra-Wide-Band (UWB) device

PROCYON-mini uses micro consumer UWB devices in Fig. 2, and the specifications of the UWB device are summarized in

Table 1. Since the communication power is low, the maximum distance of ranging and communication is limited to 300 m, which is determined from Friis's equation ⁶⁾.

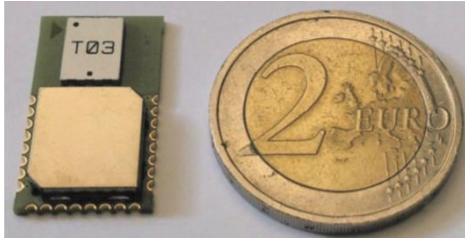


Fig. 2. Example of consumer used UWB device ⁵⁾

Table 1. Specifications of UWB device ⁵⁾

max power supply	0.23 [W]
size	23 × 13 × 2.9 [mm]
weight	1.4 [g]

The UWB device measures time of flight when a radio wave is transmitted and received, and the distance between two UWB devices is calculated from the time of flight. The period of UWB device's impulse is very short that high accurate ranging can be realized.

The standard deviation of ranging noise is changed dependent on the distance between UWB devices. The relationship is assumed as Table 2 in this paper.

Table 2. Noise property of UWB device

the distance b/w UWB devices	deviation of noise
300~200m	0.1m
200~150m	0.07m
150~100m	0.05m
100~0m	0.03m

In order to verify the proposed algorithms, a rendezvous simulator that emulates the characteristics of the UWB devices, is developed. In the simulator, three UWB devices are attached to each spacecraft (i.e., chaser and target spacecraft). In this case, when all distances between UWB devices are observed, the relative attitude is uniquely determined by the ranging data. Additionally, each spacecraft also secures redundancy of communication system and is more tolerable for a malfunction since multiple UWB devices are mounted on. Each UWB device has a half-wave dipole antenna which can be easily estimated their antenna gain. The shape of the antenna is assumed plane and the three geometric parameters are defined as Fig 3.

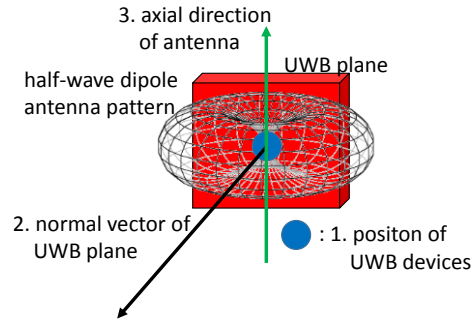


Fig. 3. Three geometric parameters of UWB device

3. Problem Setting

3.1. Estimated State Variables and Problem Setting

Firstly, estimated state variables which are needed during proximity rendezvous and docking are introduced. Four estimated state variables and sensors for the estimations are determined as Table 3.

Table 3. Observation strategies to estimate state parameters

Relative Position	Ranging with UWB
Relative Velocity	Ranging with UWB
Relative Attitude	Sharing attitude quaternion with UWB communication each spacecraft get by STT or Ranging with UWB (using multiple UWB devices)
Relative Angular Velocity	Sharing angular velocity with UWB communication each spacecraft get by Gyro sensors or Ranging with UWB (using multiple UWB devices)

3.2. Environmental Condition

Secondly, the environmental condition for the rendezvous problem is introduced. This research considers only solar radiation pressure (SRP) for a disturbance in deep space. SRP is about $4.6 \mu\text{N}/\text{m}^2$ at 1 AU. Under the configuration of the chaser and the target, the standard deviations of SRP disturbance acting on the DESTINY+ and PROCYON-mini are calculated as Table 4.

Table 4. Disturbances acting on spacecraft

Target DESTINY+	disturbance force	$0.67 \times 10^{-4} [N]$
	disturbance torque	$0.67 \times 10^{-5} [N \cdot m]$
Chaser PROCYON-mini	disturbance force	$0.33 \times 10^{-6} [N]$
	disturbance torque	$0.33 \times 10^{-7} [N \cdot m]$

3.3. State Equation and Observation Equation

Finally, the state equation and the observation equation for the proposed algorithms are discussed here. The state equation of the position and the attitude of the two spacecraft are derived. The motion of the relative position in proximity rendezvous can be assumed as a uniform linear motion because a scale of a trajectory motion in deep space is too large to consider curvilinear motions. The equation of motion of the chaser and

the target is formulated as Eq. (1) and (2).

$$M_t \dot{\mathbf{L}}_{i2t}^i = \mathbf{F}_t^i = \mathbf{F}_{td}^i + \mathbf{F}_{tm}^i \quad (1)$$

$$M_c \dot{\mathbf{L}}_{i2c}^i = \mathbf{F}_c^i = \mathbf{F}_{cd}^i + \mathbf{F}_{cm}^i \quad (2)$$

Subtracting Eq. (1) and (2), the equation of relative motion is derived. Attitude motion is obtained by Euler's rotation equation and the kinematics equation of quaternion as follows:

$$\mathbf{T}_t^b = \mathbf{I}_t \dot{\boldsymbol{\omega}}_t + \boldsymbol{\omega}_t \times \mathbf{H}^b, \quad (3)$$

$$\dot{\mathbf{q}} = \frac{1}{2} \begin{bmatrix} 0 & -\omega_x & -\omega_y & -\omega_z \\ \omega_x & 0 & \omega_z & -\omega_y \\ \omega_y & -\omega_z & 0 & \omega_x \\ \omega_z & \omega_y & -\omega_x & 0 \end{bmatrix} \mathbf{q} = \frac{1}{2} \boldsymbol{\Omega} \mathbf{q}. \quad (4)$$

The observation values of the chaser are ranging distances between UWB devices. This value can be formalized because ranging distances between UWB devices can be calculated geometrically. Considering that coordinate transformation matrixes can be derived from quaternions, the observed distance is defined as Eq. (5).

$$\text{dist}(\mathbf{U}_{cj}, \mathbf{U}_{tk}, \mathbf{L}_{c2t}^i, \mathbf{q}_{i2t}, \mathbf{q}_{i2c}) = |\mathbf{L}_{c2t}^i + \mathbf{C}_{t2i} \mathbf{U}_{tk} - \mathbf{C}_{c2i} \mathbf{U}_{cj}| \quad (5)$$

c_j and t_k represent position vectors of each UWB device which is attached on the chaser and the target. The number of j and k are changed depending on number of UWB devices.

4. Estimation of Position State when Sharing Attitude Information using UWB communication

In this paper, two estimation algorithms, which effectively use UWB's properties, are proposed. In the both algorithms, the relative position is estimated from the UWB ranging data, and the target attitude is obtained from the attitude sensor mounted on the target spacecraft via UWB communication system. The difference between the algorithms is how to get the attitude of the chaser. The first algorithm determines the chaser's attitude from the attitude sensors such as the gyro sensor and the star sensor directly. The second algorithm estimates the attitude from the multiple UWB ranging data in order to keep the estimation even if the star sensor cannot work well. This section introduces the first algorithm.

4.1. Algorithm

The first algorithm implemented in the chaser is Extended Kalman Filter (EKF) illustrated like Fig. 4.

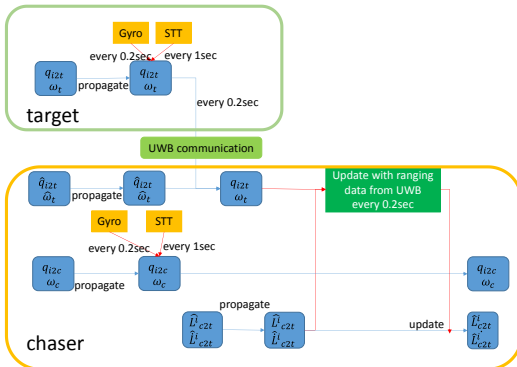


Fig. 4. First estimation algorithm of state variables using communication and ranging

The flow of the proposed algorithm is explained as follows.

1. Propagate estimated value of relative position with state equation.
2. Propagate estimated value of target's attitude and also estimates its own attitude with STT and gyro.
3. Update estimated target's attitude by getting attitude information of target with UWB communication in the period of 0.2 seconds.
4. Update relative position by EKF with UWB's ranging value in the period of 0.2 seconds. Observe matrix can be given by Jacobian because of non-linear observation equation
5. Iterate the above flow.

4.2. Simulation

4.2.1. Condition of Simulation

The conditions of the simulation are defined as Fig. 5, Table 5, and 6. The configuration of the chaser and target spacecraft is determined in reference to DESTINY+ and PROCYON-mini.

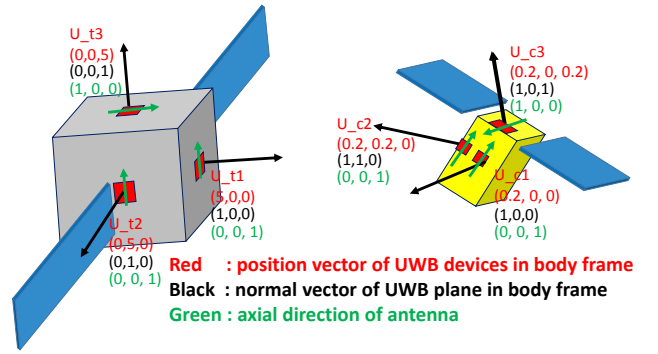


Fig. 5. Geometric parameters of the UWB devices in the simulator

Table 5. Parameter setting in the simulator

symbol	item	value	unit
deltaT	propagation time	0.1	[sec]
Q	covariance matrix of disturbance force diagonal component 1~3 row	$(0.67 \times 10^{-4})^2$	[N ²]
	diagonal component 4~6 row	$(0.33 \times 10^{-6})^2$	
M_t	mass of chaser	10	[kg]
M_c	mass of target	500	[kg]
I_c	inertia tensor of chaser	diag([0.17,0.24,0.098])	[kg m ²]
I_t	inertia tensor of target	diag([300,300,250])	[kg m ²]
STT _{time}	STT's update time	1	[sec]
UWB _{time}	UWB's update time (communication and ranging)	0.2	[sec]

Table 6. Initial value setting in the simulator

L_{c2te}^i	estimated value of relative position of target	[150,100,120]	[m]
--------------	--	---------------	-----

L_{c2t}^i	true value of relative position of target	[152,96,122]	[m]
$V_{c2t_e}^i$	estimated value of relative velocity of target	[-0.20,0.08,-0.6]	[m/s]
$V_{c2t_t}^i$	true value of relative velocity of target	[-0.70,-0.44,-0.56]	[m/s]
q_{ic2t}	true value of chaser's attitude of quaternion	[1,0,0,0]	
q_{it2t}	true value of target's attitude of quaternion	[0,0,0,1]	
ω_{c_t}	true value of chaser's angular velocity	[0,0,0]	[rad/s]
ω_{t_t}	true value of target's angular velocity	[0,0,0]	[rad/s]
P	covariance matrix of state vector	diag([36,36,36,9,9,9])	
R	covariance matrix of ranging noise of UWB devices	changing dependent on distance between UWB devices (reference to Table 1)	[m ²]

4.2.2. Results and Discussion

The estimation accuracy of the algorithm is evaluated from estimated position and velocity like Figs. 6 to 8 because the attitude information is given from the STT and the gyro sensor. Figs. 6 to 8 show that the proposed algorithm can correctly estimate the relative position and velocity. The nine ranging data obtained from the UWB devices are uniquely determined from the relative attitude and position of the chaser and the target. In addition, because the attitude information of each spacecraft is shared by the UWB communication, the estimated relative position between spacecraft can be directly obtained from the nine ranging data. Therefore, the observability of the algorithm is assured sufficiently. Finally, the convergence of position estimation leads to accuracy of velocity estimation.

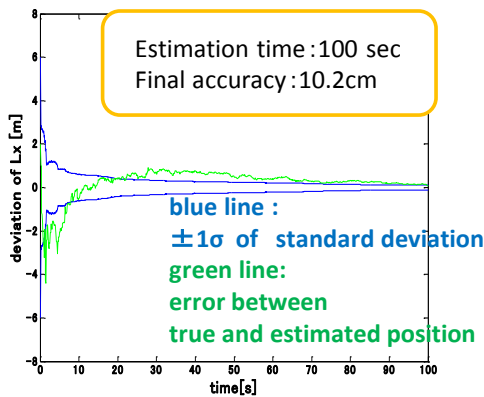


Fig. 6. Standard deviation of x component of relative position of target from the standpoint of chaser

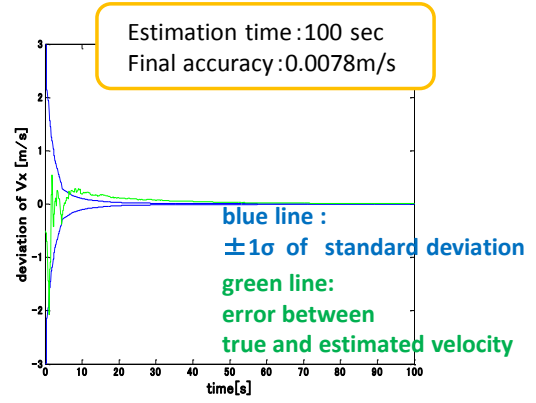


Fig. 7. Standard deviation of x component of relative velocity of target from the standpoint of chaser

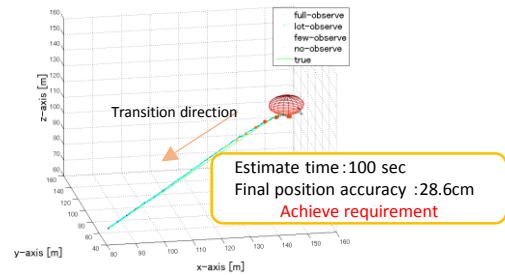


Fig. 8. Time transition of true and estimated relative position of target from the standpoint of chaser, and error ellipsoid.

One of the difference vectors between true and estimated position is shown in Eq. (6). It is required that the final misalignment of positions of PROCYON-mini and DESTINY+ just before docking is within 0.3 m. Therefore, this result achieves required accuracy of position estimation.

$$\Delta L_{c2t}^i = \begin{bmatrix} 0.1028 \\ 0.1409 \\ -0.2272 \end{bmatrix} \text{ [m]} \quad (6)$$

In order to confirm the estimation accuracy, a Monte Carlo analysis is performed 50 times. In the analysis, the error norm between initial estimated position and true position is set as 6 m and is distributed randomly. The result of the analysis is illustrated as Fig. 9. This figure verifies that the estimation accuracy of the proposed algorithm satisfies the required

accuracy.

5. Simultaneous Estimation of Relative Position and Attitude of Chaser

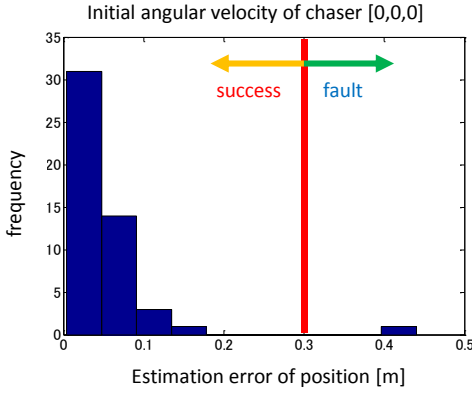


Fig. 9. Result of the Monte Carlo simulation for the first algorithm

In section 4, the attitude information of chaser is obtained by the chaser's STT and gyro sensor. However, the STT cannot be used in some cases as follows.

1. Attitude cannot be determined when field of view of STT is pointed to the target spacecraft.
2. STT has to be avoided from sun keep out angle.(35 degree from FOV direction)
3. large angular velocity (0.5 deg/s over)

Therefore, in this section, the second estimation algorithm that estimates the attitude by using multiple UWB devices are proposed and discussed. In this algorithm, the attitude of chaser is added to estimation variables from the previous algorithm in section 4. The added variables are estimated by using ranging data of the multiple UWB devices. The attitude state variables of target are given by the communication when ranging simultaneously.

5.1. Algorithm

The proposed algorithm in this section is illustrated in Fig. 10. The attitude quaternion of the chaser with regards to inertial frame is the parameter of observation equation. It is given a partial derivative to get Jacobian for observation matrix.

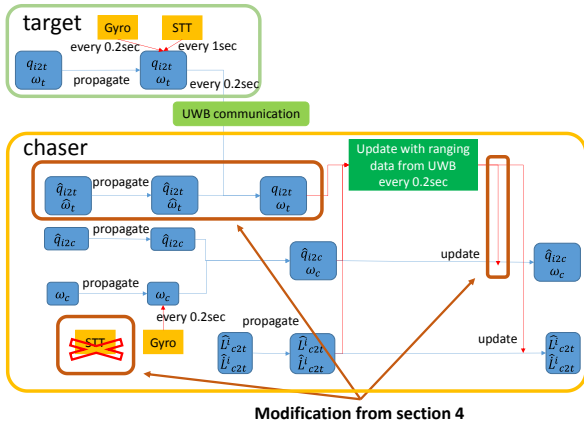


Fig. 10. Simultaneous estimation algorithm of relative position and chaser's attitude.

5.2. Simulation

5.2.1. Condition of Simulation

The simulation conditions for the quaternion estimation are added to the conditions mentioned in the previous section. In addition, the covariance matrix of state vector is also expanded as Table 7.

Table 7. Specifications of added or changed state variables

q_{i2c_t}	estimated quaternion of chaser's attitude	[0.9774,0.1222, 0.1222,0.1222]
tf	total simulation time	200
P	covariance matrix of state vector	diag([36,36,36,9,9,0, 1,0,1,0,1,0,1])

In this numerical experiment, the initial angular velocity of chaser is changed in three cases. The three estimation results are compared to discuss the optimal angular velocity of chaser.

Table 8. Three patterns of angular velocity

slow spin case	$[\pi/100, \pi/200, \pi/300]$ [rad/s]
fast spin case	$[\pi/10, \pi/20, \pi/30]$ [rad/s]
non-spin case	[0,0,0] [rad/s]

5.2.2. Results and Discussion

The simulation results are shown in Figs. 11 to 16. These results reveal that the most accurate estimation is fulfilled in the slow spin case. The estimation of the slow spin case is stable and fast. However, in the fast spin case, the estimation is vibrating, and it decreases estimation accuracy. In the non-spin case, estimation accuracy is good but the speed of convergence is slow. It is considered that these differences of the results are caused by the observability of the proposed algorithm. It is discussed in the section.

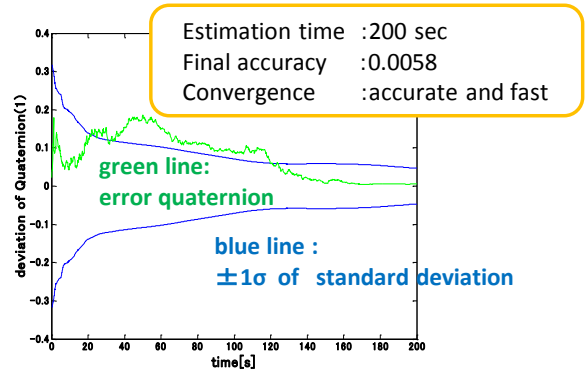


Fig. 11. Standard deviation of the slow spin case (first component of the error quaternion)

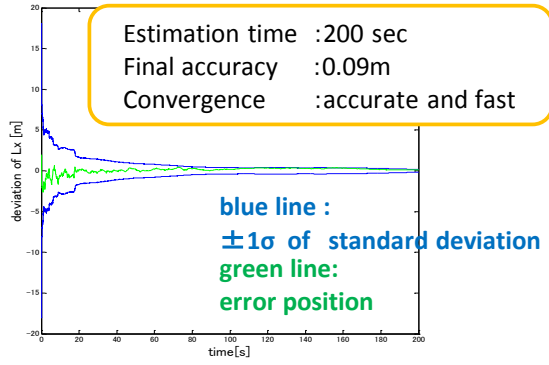


Fig. 12. Standard deviation of the slow spin case (x component of the error position)

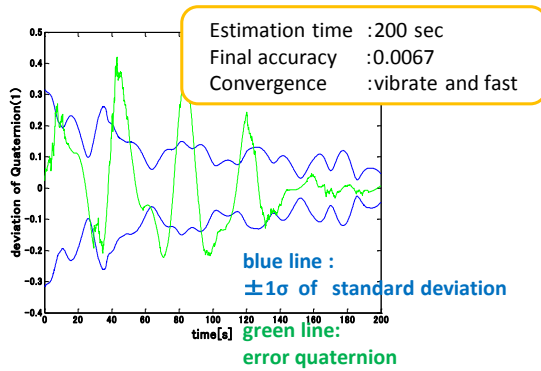


Fig. 13. Standard deviation of the fast spin case (first component of the error quaternion)

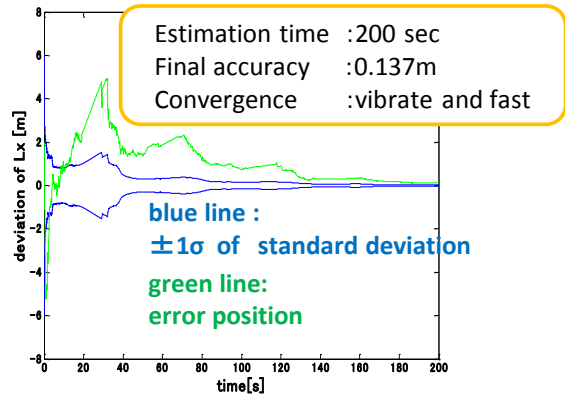


Fig. 14. Standard deviation of the fast spin case (x component of the error position)

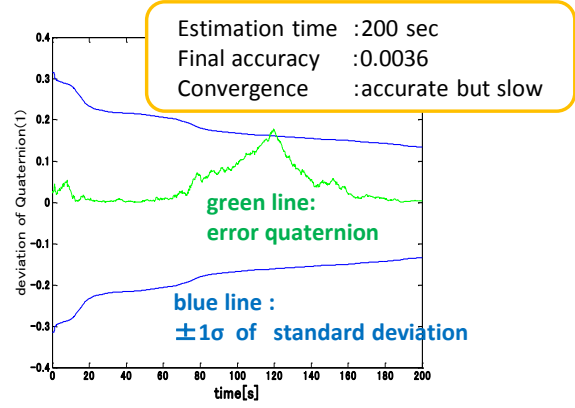


Fig. 15. Standard deviation of the non-spin case (first component of the error quaternion)

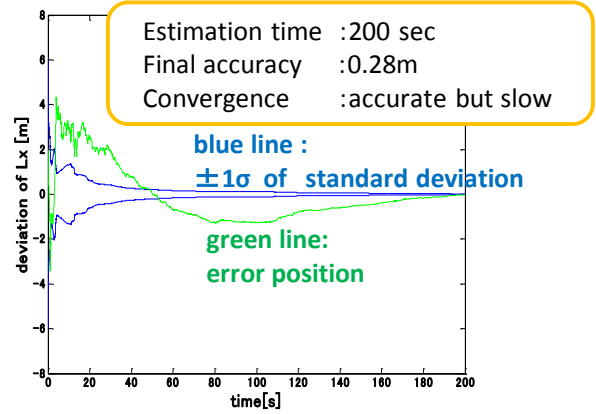


Fig. 16. Standard deviation of the non-spin case (x component of the error position)

In order to confirm the observability of the estimation algorithm, the rank of observation matrix is calculated. The state transition matrix and the observation matrix is formalized as Eq. (7), and Eq. (8), respectively.

$$A = \begin{bmatrix} \mathbf{0} & E & \mathbf{0} \\ \mathbf{0} & \mathbf{0} & \mathbf{0} \\ \mathbf{0} & \mathbf{0} & \Omega \end{bmatrix} \quad (7)$$

$$H = [H_1 \quad \mathbf{0} \quad H_2] \quad (8)$$

Calculating the observation matrix, 10th to 18th line of the matrix is represented as Eq. (9).

$$HA = [\mathbf{0} \quad H_1 \quad H_2\Omega], \quad (9)$$

where Ω is in Eq. (4). When angular velocity is zero, $H_2\Omega$ will be zero matrix. This shape of matrix degrades the rank of the observation matrix to 9 from 10 (the full rank of the observation matrix). In other words, the system becomes non-observable. It is thought that the angular velocity makes the attitude variation of the chaser, and several ranging observations under different geometric situations can be obtained in the estimation process. These different observations enhance the observability of this system.

From Eq. (9), it is verified that the slow spin case has the observability, and then the position and attitude can be estimated simultaneously. Fig. 12 shows that the standard deviation is converged in 200 seconds. It is indicated that the nine ranging data are sufficient to estimate position and attitude

by the slow spin.

In the fast spin case, sufficient angular velocity makes observability matrix full-rank. However, since the chaser's rotation is too strenuous, the chaser's UWB devices are faced away from the target's UWBs and no ranging information can be observed. Then, the estimation results vibrate, and the estimation accuracy is worse than that of the slow spin case.

In the non-spin case, the chaser has almost zero angular velocity because the chaser receives only a small disturbance of SRP. Then, the observability is ineffective, and convergence of the standard deviation of quaternion is slower than that of the slow spin case. However, in this case, the state variables of attitude quaternion begin to converge rapidly from 120 seconds. This is concluded that the distance between the chaser and the target is below 100 m and the noise of ranging data from UWB devices is changed smaller mentioned in Table 2. Therefore, the estimation accuracy can be improved by reducing noise of ranging in spite of ineffective observability.

In order to verify the appropriate angular velocity of the chaser, a Monte Carlo analysis is performed. In the analysis, the initial angular velocity of chaser and ranging noise of UWB devices are given randomly in order to evaluate attitude estimation error angle. The result is shown in Fig. 17. This figure shows that the slow spin case improves the estimation accuracy of attitude independent of the ranging noise. However, the estimation accuracy in the fast spin case and the non-spin case depends on the ranging noise. This numerical experiment quantitatively verifies the qualitative analysis of this section.

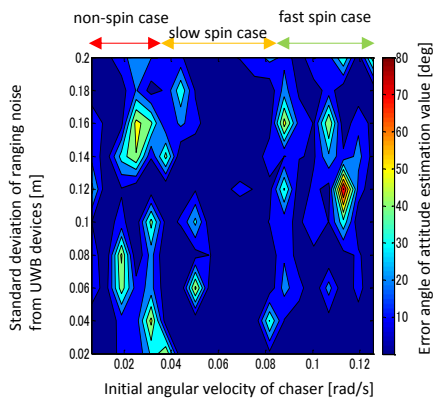


Fig. 17. The simulation for evaluating error angle of attitude estimation

6. Conclusion

In this research, two estimation algorithms of relative position and attitude by using UWB devices are proposed to realize rendezvous and docking between micro and medium spacecraft in deep space.

The first algorithm estimates relative position by using ranging data from the UWB devices, and determines the relative attitude by using the attitude sensors mounted on each spacecraft. The attitude information of the target is shared with

the chaser via the UWB communication system. Due to the attitude sharing system, the relative position can be directly estimated from the multiple ranging data of the UWB devices. Hence, this algorithm ensures the observability and provides the accurate and stable estimation.

The second algorithm additionally estimates the chaser's attitude by using multiple ranging data from UWB devices under the assumption that the chaser's STT cannot work well. In this algorithm, the relative angular velocity and position influence the observability and the estimation accuracy respectively. The Monte Carlo analysis shows the appropriate relative angular velocity and position for accurate and stable estimation. To keep the appropriate condition, a rendezvous control algorithm should be investigated. The analysis contributes to planning the orbital and attitude maneuver of interplanetary proximity rendezvous and docking.

The estimation algorithms and the analysis results discussed in this paper will expand the capability of interplanetary mission by micro spacecraft.

Acknowledgments

This research was supported by Prof. Shinichi Nakasuka, Assoc. Prof. Ryu Funase, and Mr. Satoshi Ikari in the University of Tokyo. This research was also supported by Assistant Prof. Tomiki in ISAS/JAXA for UWB devices. I would like to express my gratitude to all DESTINY+ and PROCYON-mini project team members.

References

- 1) Yuya Nakayama *et al.* "University of Tokyo's Ongoing Student-Lead Pico-Satellite Projects -Cubesat XI and PRISM", 55th International Astronautical Congress, Vancouver, 2004,
- 2) Miyamura, N. *et al.* "High Resolution Extensible Telescope for University of Tokyo's Remote Sensing NanoSatellite PRISM", 25th International Symposium on Space Technology and Science, ISTS Paper 2006-n-20, 2006.
- 3) Funase, R., *et al.*: 50kg-class Deep Space Exploration Technology Demonstration Micro-spacecraft PROCYON, 8th Small Satellites Conference, SSC14-VI-3, 2014.
- 4) Funase, R., *et al.*: Close Flyby Observation of An Asteroid by A Small Probe PROCYON-mini and Rendezvous Docking Experiment in Deep Space, Journal of the Japan Society for Aeronautical and Space Sciences 60, 2016 (in Japanese).
- 5) Source of error in DW1000 based two-way-ranging (TWR) schemes, <http://www.decawave.com/sites/default/files/product-pdf/dwm1000-product-brief.pdf>. (accessed January 26, 2017).
- 6) Harald T. Friis, "A note on a simple transmission formula" *Proceedings of the I.R.E. and Waves and Electrons 1946* pp.254.
- 7) Fehse, W., *Automated rendezvous and docking of spacecraft*, Cambridge Univ. Press, Cambridge, England, U.K., 2003, pp. 171-215.
- 8) Source of error in DW1000 based two-way-ranging (TWR) schemes, http://www.decawave.com/sites/default/files/resources/aps011_source_s_of_error_in_twr.pdf. (accessed January 26, 2017).
- 9) Son-Goo Kim, John L. Crassidis, Yang Cheng, Adam M. Fosbury, "Kalman Filtering for Relative Spacecraft Attitude and Position Estimation", *JOURNAL OF GUIDANCE, CONTROL, AND DYNAMICS*, vol.30, No.1, January-February 2007.